



The synthesis and characterization of a series of cobalt(II) β -ketoaminato complexes and their cytotoxic activity towards human tumor cell lines

Lydia Gurley^a, Natalia Beloukhina^b, Kalun Boudreau^b, Andis Klegeris^{b,*}, W. Stephen McNeil^{a,*}

^a Department of Chemistry, University of British Columbia Okanagan, 3333 University Way, Kelowna, British Columbia, Canada, V1V 1V7

^b Department of Biology, University of British Columbia Okanagan, 3333 University Way, Kelowna, British Columbia, Canada, V1V 1V7

ARTICLE INFO

Article history:

Received 10 November 2010

Received in revised form 16 February 2011

Accepted 14 March 2011

Available online 22 March 2011

Keywords:

Cobalt complexes

Fluorinated ligands

Cytotoxic activity

Caspase-3

MAP kinases

Reactive oxygen species

ABSTRACT

A series of square planar cobalt(II) compounds bearing tetradentate β -ketoaminato ligands with variation in the number of $-\text{CF}_3$ ligand substituents has been prepared and structurally and spectroscopically characterized. The fluorinated β -ketoamine ligands were prepared utilizing a multistep reaction sequence employing a silylenol protecting group. An additional tetrahedral cobalt compound bearing two bidentate β -ketoaminato ligands was also prepared and characterized.

Cytotoxic activity of the cobalt-containing complexes was evaluated using six human cell lines; including two different prostate cancer cell lines (PC-3 and VCaP), acute monocytic leukemia (THP-1), astrocytoma (U-373 MG), hepatocellular carcinoma (HepG2), and neuroblastoma (SH-SY5Y) cells. The cobalt compounds are more active than their corresponding ligands. The activity is cell type specific; the cobalt compounds exhibit strong activity against human prostate cancer and monocytic leukemia cells but weak or no activity against neuroblastoma, astrocytoma, and liver carcinoma cells. Activity generally increases with a greater number of $-\text{CF}_3$ substituents, and square planar complexes exhibit greater activity than the tetrahedral derivative. The mechanisms of activity against human PC-3 prostate cancer cells involve caspase-3 and two different mitogen-activated protein kinases. The addition of a thiol antioxidant reduced cytotoxicity, suggesting the possible involvement of reactive oxygen species. These cobalt complexes may represent a novel class of cytotoxic drugs selective towards certain types of tumors.

© 2011 Elsevier Inc. All rights reserved.

1. Introduction

Inorganic and bioinorganic medicinal agents have made a growing contribution to medical science and human health in the past half century [1]. Arguably, the most widely known inorganic therapeutic agent is *cis*-diamminedichloroplatinum(II) (cisplatin) and its derivatives carboplatin and oxaliplatin. Cisplatin and carboplatin have been in widespread use for many years in the treatment of several forms of cancer, including ovarian, cervical, head and neck, and non-small-cell lung cancers [2]. However, it presents the greatest success against testicular cancer for which the overall cure rate exceeds 90%, and is nearly 100% for early-stage disease [3]. The success of these compounds as solid tumor therapeutics has fostered a great deal of research into the development and improvement of platinum-based drugs [4–8]. In contrast, and despite the known biological roles of cobalt as found in cobalamins [9] and cobalt nitrile hydratases [10], relatively few studies have examined the potential therapeutic properties of cobalt compounds. Ott et al. have reported the synthesis and antitumor efficacy of [2-acetoxy-(2-propynyl)benzoate] hexa-

carbonyldicobalt [11]. Its mode of activity against cancer cells is unknown but it has been suggested that these complexes may interact with DNA or DNA-related cellular biochemical pathways [12]. A number of cobalt(III) complexes have been examined for their antiviral properties, with the most significant development being the approval of Doxovir as a topical microbicide for the treatment of herpes simplex virus type 1 [13].

Although organofluorine compounds are virtually absent as natural products, 20–25% of drugs in pharmaceutical development contain at least one fluorine atom [14]. Introduction of fluorine atoms into a structure can dramatically change the physical and chemical properties of a complex, including its potential pharmaceutical behavior [15]. In this paper we present a series of cobalt compounds bearing primarily tetradentate bis(β -ketoaminato) ligands, with variation in the number of $-\text{CF}_3$ ligand substituents. The tetradentate ligands enforce a square-planar geometry for these complexes. One cobalt compound bears two bidentate ligands and a tetrahedral geometry, permitting an analysis of the effect of complex geometry on the cytotoxic activity profile. The proligands and their corresponding cobalt complexes are presented in Fig. 1.

Preliminary experiments aimed at evaluating possible biological activities of the newly synthesized compounds indicated cytotoxic activity of the cobalt-containing complexes. More detailed studies

* Corresponding authors. Tel.: +1 250 807 8751; fax: +1 250 807 8005.

E-mail addresses: andis.klegeris@ubc.ca (A. Klegeris), s.mcneil@ubc.ca (W.S. McNeil).

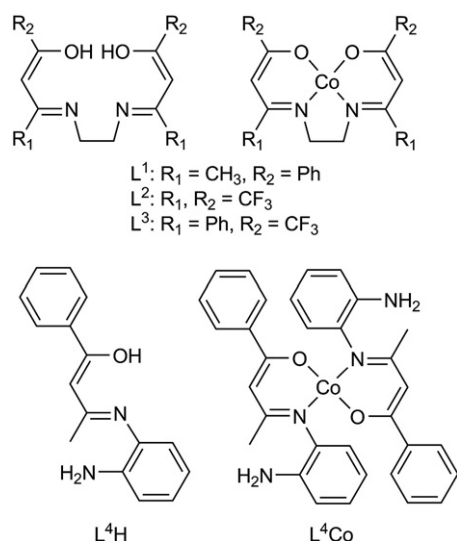


Fig. 1. Structures of β -ketoamino ligands and corresponding cobalt complexes described in this study.

were designed to establish the half-maximal effective concentration (EC_{50}) values for the cobalt compounds against six different human tumor cell lines including PC-3 (prostate), VCaP (prostate), THP-1 (acute monocytic leukemia), U-373 MG (astrocytoma), HepG2 (liver carcinoma) and SH-SY5Y (neuroblastoma). We also measured the activity of the ligands used in preparation of the metal complexes. These experiments aimed to determine: 1) whether there was a difference in the cytotoxic activity between the organic ligands and their corresponding metal complexes; 2) whether alterations in the peripheral ligand substituents had an effect on the activity of the compounds; and 3) whether the activity associated with the different compounds was cell type specific. We performed an additional series of experiments to elucidate the molecular mechanisms underlying the cytotoxic activity of the cobalt-containing drugs. It has been reported previously that anti-tumor drug action is often associated with apoptotic processes involving activation of caspases [16], mitogen-activated protein (MAP) kinases [16,17] and/or generation of reactive oxygen intermediates [18]. This article presents experimental evidence supporting involvement of caspase-3, two different MAP kinases, and reactive oxygen intermediates in the cytotoxic activity of cobalt-containing drugs toward human PC-3 prostate adenocarcinoma cells.

2. Experimental procedure

2.1. Materials and methods

Anhydrous solvents were purified in Glass Contour solvent purification towers, including hexanes (ACS reagent, Fisher, Waltham, MA, USA), diethylether (anhydrous, VWR, West Chester, PA, USA), and tetrahydrofuran (THF, HPLC grade, Fisher). Methanol, ethanol, and toluene were used as received (ACS, Fisher). CoCl_2 , sodium bis(trimethylsilyl) amide ($\text{Na}[\text{N}(\text{SiMe}_3)_2]$), sodium hydride, *tert*-butyldimethylchlorosilane, 1,2-diaminoethane, 4,4,4-trifluoro-1-phenyl-1,3-butanedione, 1-phenyl-1,3-butanedione, and 1,2-phenylenediamine were all purchased from Sigma-Aldrich (St. Louis, MO, USA) and used as received. Hexafluoroacetylacetone (Sigma-Aldrich) was thrice freeze-pump-thaw degassed before use. CDCl_3 (99.6+ atom% D) was dried over P_2O_5 , distilled under reduced pressure, freeze-pump-thaw degassed, and stored under dinitrogen. Bis(benzoylacetone)ethylenediimine ($L^1\text{H}_2$) and the corresponding complex (bis(benzoylacetone)ethylenediimino)cobalt(II) ($L^1\text{Co}$) were prepared by the previously reported procedures and have been fully characterized

[19–21]. $\text{Co}(\text{N}(\text{SiMe}_3)_2)_2 \cdot \text{THF}$ was prepared according to the published procedure [22]. All reactions were carried out in an inert atmosphere glove box or on a vacuum/nitrogen line using standard air-sensitive Schlenk techniques.

The following substances were used in various assays and were obtained from Sigma-Aldrich: diaphorase (EC 1.8.1.4, from *Clostridium kluyveri*); dimethyl sulfoxide (DMSO); sodium L-lactate; sodium oxamate; p-iodonitrotetrazolium violet; NAD^+ ; 3-(4,5-dimethylthiazol-2-yl)-2,5-diphenyltetrazolium bromide (MTT); N-acetyl-L-cysteine (NAC), an antioxidant; SP600125, a selective inhibitor of c-Jun NH2-terminal kinase (JNK); and PD98059, a selective cell-permeable inhibitor of MAP kinase (MAPK)/extracellular signal-regulated kinase (ERK) kinase (MEK)1/2. An Alexis caspase-3 fluorometric assay kit was purchased from Enzo Life Sciences (Plymouth Meeting, PA, USA).

2.1.1. Characterization of compounds

^1H and ^{19}F NMR data were collected on a Varian 400 MHz NMR spectrometer at room temperature in J. Young valve NMR tubes. ^1H NMR chemical shift values were calibrated relative to residual protio-solvent signals, and ^{19}F NMR signals were referenced to external CF_3COOH . X-ray crystallographic analyses were performed by Brian Patrick at the University of British Columbia, Vancouver, BC, Canada. Elemental analysis was performed by Guelph Chemical Laboratories of Guelph, Ontario, Canada.

2.1.2. Cell culture

The following human cell lines were obtained from the American Type Culture Collection (ATCC, Manassas, VA, USA): PC-3 prostate adenocarcinoma; VCaP prostate cancer epithelial cell line; THP-1 acute monocytic leukemia; U-373 MG astrocytoma; and HepG2 hepatocellular carcinoma. The human neuroblastoma SH-SY5Y cell line was a gift from Dr. R. Ross, Fordham University, NY. Cells were grown in Dulbecco's modified Eagle's medium-nutrient mixture F12 ham (DMEM-F12) supplemented with 10% fetal bovine serum (FBS) supplied by Thermo Scientific HyClone (Logan, UT, USA). All cell lines were used without initial differentiation.

2.2. Syntheses

2.2.1. Synthesis of bis(hexafluoroacetylacetone)ethylenediimine ($L^2\text{H}_2$)

$L^2\text{H}_2$ was prepared via a modification of a previously described procedure [23]. In a glovebox, hexafluoroacetylacetone (7.45 g, 35.8 mmol) was cooled to -35°C . Sodium hydride (0.859 g, 35.8 mmol) was predissolved in THF and cooled to -35°C . The cold hexafluoroacetylacetone and sodium hydride solutions were added alternatively in small portions to 20 mL THF, with the mixture kept cold with an acetone/liquid N_2 bath during these additions. Extensive, somewhat violent effervescence occurred. The mixture was allowed to warm to ambient temperature and stirred overnight, resulting in a clear, slightly pink mixture. The flask was removed from the glovebox and attached to the vacuum line. *tert*-Butyldimethylchlorosilane (5.40 g, 35.8 mmol) dissolved in 5 mL anhydrous THF was added to a pressure-equalized addition funnel. The *tert*-butyldimethylchlorosilane solution was added very slowly to the deprotonated ketone solution. After complete addition, the mixture was refluxed overnight to give a yellow solution with a beige precipitate. The solution was cannulated through Celite to give a clear yellow solution. In a separate flask 1,2-diaminoethane (0.652 g, 10.9 mmol) was dissolved in 5 mL anhydrous THF. The two separate solutions were cooled in an acetone/ N_2 bath. The 1,2-diaminoethane solution was cannulated into the protected ketone solution. After complete addition, the reaction was allowed to warm to room temperature and resulted in a cloudy white suspension. After 1 h of stirring, the THF was removed under reduced pressure to give a mixture of white and pink solids. The solids were redissolved in 20 mL methanol giving a pink solution that was refluxed for 3 h. Cooling the solution resulted in the deposition of a

white solid. The solution was filtered to collect 1.985 g (41.1%) of white solid. ^1H NMR (400.13 MHz, CDCl_3) δ 10.58 (s, 1H), 5.87 (s, 1H), 3.79 (s, 2H). ^{19}F NMR (376.50 MHz, CDCl_3) δ -77.41 (s), -66.49 (s).

2.2.2. Synthesis of (benzoyltrifluoroacetone)ethylenediimine (L^3H_2)

L^3H_2 was synthesized following the same procedure as outlined for L^2H_2 utilizing 4,4,4-trifluoro-1-phenyl-1,3-butanedione in place of hexafluoroacetylacetone, to afford L^3H_2 as white crystals in 60.0% yield. ^1H NMR (400.13 MHz, CDCl_3) δ 10.93 (s, 1H), 7.46 (s, 3H), 7.18 (s, 2H), 5.44 (s, 1H), 3.43 (s, 2H). ^{19}F NMR (376.50 MHz, CDCl_3) δ -70.65 (s).

2.2.3. Synthesis of (benzoylacetone)phenyleneimineamine (L^4H)

1-Phenyl-1,3-butanedione (2.013 g, 12.49 mmol) was dissolved in 30 mL toluene to give a yellow solution. 1,2-Phenylenediamine (0.6757 g, 6.248 mmol) was added directly and the solution was refluxed overnight using a Dean-Stark apparatus. The resulting bright orange solution was concentrated. Hexane was added and the mixture was placed in the freezer at -35°C overnight. The solution was filtered to give an orange solid, recrystallized from ethanol to yield 1.264 g (80.23%) of yellow crystals. ^1H NMR (400.13 MHz, CDCl_3) δ 12.47 (s, 1H), 7.94–7.89 (m, 2H), 7.49–7.39 (m, 3H), 7.13–7.01 (m, 2H), 6.81–6.71 (m, 2H), 5.93 (s, 1H), 3.89 (s, 2H), 1.99 (s, 3H).

2.2.4. Synthesis of

(bis(hexafluoroacetylacetonato)ethylenediimino)cobalt(II) (L^2Co)

L^2H_2 (0.1678 g, 0.0291 mmol) was dissolved in 5 mL THF. In a separate vial $\text{Co}(\text{N}(\text{SiMe}_3)_2)_2 \cdot \text{THF}$ (0.1104 g, 0.0291 mmol) was dissolved in 5 mL THF. Dropwise addition of the L^2H_2 solution to that of $\text{Co}(\text{N}(\text{SiMe}_3)_2)_2 \cdot \text{THF}$ resulted in an immediate color change to a dark red mixture. After approximately 2 min, orange solid precipitated from the solution. The reaction was allowed to stir overnight. The solvent was removed *in vacuo* to yield 0.3934 g (79.14%) of a very dark red solid. The red solid was redissolved in hexanes giving a dark orange solution. The solution was filtered through Celite then placed in the freezer at -35°C overnight to induce the development of analytically-pure bright orange crystals. ^1H NMR (400.13 MHz, CDCl_3) δ +116.45 (s, 2H), -91.65 (s, 1H). EA analysis; calculated: C 28.99, H 1.22, N 5.64; found: C 29.40, H 1.20, N 5.96.

2.2.5. Synthesis of (bis(benzoyltrifluoroacetone)ethylenediimino)cobalt(II) (L^3Co)

L^3H_2 (0.4953 g, 1.085 mmol) was dissolved in 5 mL diethylether resulting in a creamy white suspension. In a separate vial, $\text{Co}(\text{N}(\text{SiMe}_3)_2)_2 \cdot \text{THF}$ (0.3172 g, 1.096 mmol) was dissolved in 2 mL diethylether. Dropwise addition of the L^3H_2 suspension to the $\text{Co}(\text{N}(\text{SiMe}_3)_2)_2 \cdot \text{THF}$ solution resulted in an immediate color change to light orange, which then grew progressively darker orange. The solution was stirred overnight and the solvent was removed *in vacuo* to yield 0.4937 g (88.65%) of orange solid. The solid was redissolved in diethylether and filtered through Celite. The solution was placed in the freezer at -35°C to induce deposition of analytically-pure red crystals. ^1H NMR (400.13 MHz, acetone- d_6) δ +100.97 (s, 1H), +29.41, +15.37, +9.55, -62.82 (s, 2H). EA analysis; calculated: C 51.47, H 3.14, N 5.46; found C 51.45, H 2.96, N 5.38.

2.2.6. Synthesis of [(benzoylacetone)phenyleneimineamino]cobalt(II) (L^4Co)

L^4H (0.4185 g, 1.659 mmol) was dissolved in 10 mL diethylether, resulting in a yellow solution. $\text{Co}(\text{N}(\text{SiMe}_3)_2)_2 \cdot \text{THF}$ (0.304 g, 0.802 mmol) was dissolved in 5 mL diethylether and the resulting dark green solution was added dropwise to the ligand solution. The mixture immediately changed to a dark orange color with a dark orange precipitate. The mixture was stirred overnight. The solvent was removed *in vacuo* to yield 0.4757 g (85.08%) of orange solid. The solid was redissolved in THF/hexanes and filtered through Celite. The filtrate was placed in the freezer at -35°C to induce the formation of X-ray quality

dark orange crystals. ^1H NMR (400.13 MHz, CDCl_3) δ 18.45, 14.74, 12.68, 10.52, 9.88, -10.95, -19.22, -26.46, -34.83, -54.72. EA analysis; calculated: C 68.45, H 5.38, N 9.98; found C 67.43, H 5.59, N 9.38.

2.3. *In vitro* assays

2.3.1. Caspase assay

The enzymatic activity of caspase-3 was measured fluorometrically by using an assay kit purchased from Enzo Life Sciences. The assay was carried out according to the instructions supplied by the manufacturer as described before [24]. PC-3 cells were seeded into 60 mm tissue culture dishes (Corning, NY, USA) at a concentration of 1.5×10^5 cells/mL in 20 mL of DMEM-F12 medium containing 5% FBS. L^1Co (5–25 μM), L^2Co (1–10 μM) or DMSO aliquots were added and cells incubated for 48 h followed by cell lysis. Caspase-3 activity in cell lysates was expressed in Fluorescence Units per g protein. Protein concentrations in the samples were measured by using the Bradford reagent and bovine serum albumin solutions to generate a standard curve [25].

2.3.2. Cell toxicity assays

Various human cell lines were seeded into 24-well plates at the following concentrations: PC-3 at 1.5×10^5 cells/mL; VCaP at 1.5×10^5 cells/mL; THP-1 at 5.0×10^5 cells/mL; SH-SY5Y at 2.0×10^5 cells/mL; U-373 MG at 2.0×10^5 cells/mL; and HepG2 at 5.0×10^4 cells/mL. 0.4–0.8 mL of DMEM-F12 medium containing 5% FBS was used to plate out the required number of cells. All cell types, except non-adherent THP-1 cells, were allowed to adhere for 24 h at 37°C in a CO_2 incubator (humidified 5% CO_2 and 95% air atmosphere). Subsequently, cell medium was replaced with fresh medium and cells incubated in the presence or absence of various compounds (1–50 μM) or their vehicle solution (DMSO) for further 48 h. Concentration of DMSO was kept at 0.5% in all samples. MAPK inhibitors (20 μM) or various concentrations of NAC were added 15 min prior to the addition of the newly synthesized compounds. Following the incubation, 100 μL of cell culture media was sampled for lactate dehydrogenase (LDH) to determine the percentage of dead cells, while the evaluation of surviving cells was performed by the MTT assay as previously described [26].

The MTT assay is based on the ability of viable, but not dead cells, to convert the tetrazolium salt (MTT) to colored formazan. The viability of SH-SY5Y cells was determined by adding MTT to the SH-SY5Y cell cultures to reach a final concentration of 0.5 mg/mL. Following a 1 h incubation period at 37°C , the dark crystals which had formed were dissolved by adding to the wells an equal volume of SDS/DMF extraction buffer (20% sodium dodecyl sulfate, 50% N,N-dimethyl formamide, pH 4.7). Subsequently, the plates were placed overnight at 37°C , after which 100 μL aliquots were transferred to 96-well plates and optical densities at 570 nm were measured using a microplate reader. The viable cell value was calculated as a percentage of the value obtained from cells incubated with fresh medium only.

LDH activity in cell culture supernatants was measured by an enzymatic test in which formation of the formazan product of iodonitrotetrazolium dye was followed colorimetrically. 100 μL of cell culture supernatant from each sample was pipetted into a 96-well plate, followed by addition of 15 μL lactate (36 mg/mL) and 15 μL *p*-iodonitrotetrazolium violet (2 mg/mL) solutions into each well. The enzymatic reaction was started by addition of 15 μL of NAD^+ /diaphorase solution (3 mg/mL NAD^+ ; 2.3 mg solid/mL diaphorase). After a 15–30 min incubation period, the reaction was terminated by the addition of 15 μL of oxamate (16.6 mg/mL) into each well. Optical densities at 490 nm were measured by a microplate reader. The amount of LDH released was expressed as a percentage of the value obtained in comparative wells in which cells were completely lysed by 1% Triton X 100.

2.3.3. Statistical analysis

Data are presented as means \pm standard error of the mean (SEM). The concentration-dependent effects of various compounds *in vitro*

were evaluated statistically by the randomized block design analysis of variance (ANOVA) followed by Fisher's least significant differences (LSD) *post hoc* test. The P values obtained by paired Student's *t* test were corrected for multiple comparisons by Holm's step-down method [27].

3. Results and discussion

3.1. Ligand synthesis

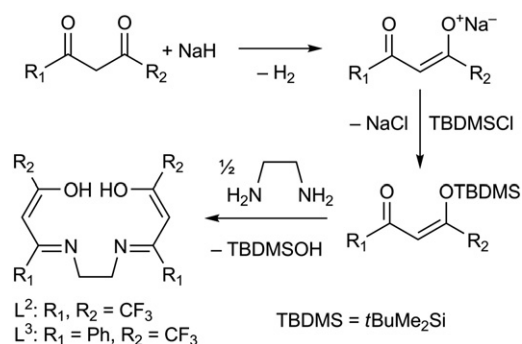
The non-fluorinated proligand L^4H (see Fig. 1) is easily prepared via the Schiff base condensation of 1-phenyl-1,3-butanedione and 1,2-diaminoethane in refluxing toluene, using a Dean-Stark apparatus. However, attempts to prepare fluorinated β -ketoimines in which one or two of the R groups are fluoroalkyl groups have been shown to be unsuccessful via Schiff base condensation reactions [23,28], so the synthesis of the fluorinated proligands L^2H_2 and L^3H_2 cannot employ this method. It has been suggested that this synthetic approach is not viable due to the high acidity of the fluorinated β -diketones, which leads to protonation of the diamine and formation of a diketone ammonium salt, preventing the desired condensation reaction [28]. A synthesis has been reported in which sublimation of the ammonium salt does afford the L^2H_2 complex, but the product is isolated in low yield due to formation of a cyclic byproduct in which both diketone oxygen atoms have reacted with the same diamine molecule [29]. A different synthetic methodology for the preparation of the desired fluorinated proligands was therefore adopted [23].

To overcome the problem associated with the protonation of the diamine, the appropriate diketone was first deprotonated using NaH under anhydrous conditions to produce $[R_1COCHCOR_2]^- Na^+$. This salt was subsequently treated with *tert*-butyldimethylchlorosilane to produce a silylenoether, which is treated with 1,2-diaminoethane to form the desired fluorinated β -ketoimine. The silyl moiety acts as a protecting group to ensure that the amine condensation occurs at only one of the carbonyl groups of the diketone, and thereby prevents the formation of a cyclic product. This synthetic approach was successful in the preparation of the proligands L^2H_2 and L^3H_2 (Scheme 1).

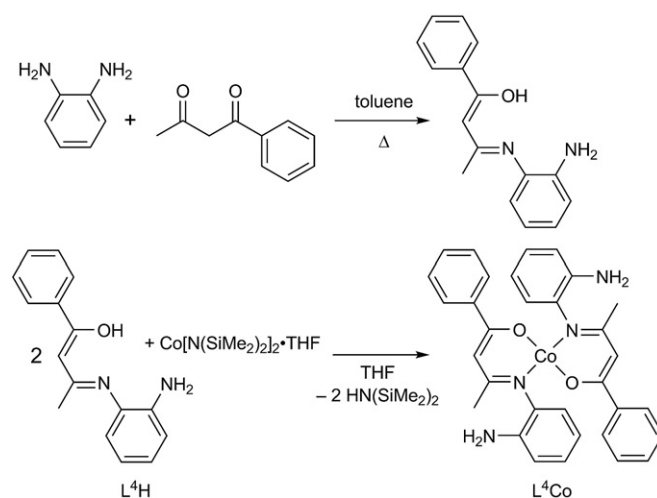
In an attempt to prepare the phenylene derivative of L^1H_2 , a similar Schiff base condensation reaction was performed reacting 1-phenyl-1,3-butanedione and 1,2-phenylenediamine. The reaction proceeded in a 1:1 ratio rather than a 2:1 ratio, resulting in proligand L^4H and subsequently complex L^4Co (Scheme 2).

3.2. Cobalt complex syntheses

L^1Co is readily prepared via the established procedure by adding L^1H_2 to simple cobalt salts such as $CoCl_2$ or $Co(OAc)_2$ in the presence of base [19–21]. Such an approach is not successful for L^2Co , L^3Co , and L^4Co . A new synthetic approach was adopted using the diamide salt $Co(N(SiMe_3)_2)_2 \cdot THF$. Burger and Wannagat [22] reported the successful preparation of the cobalt amido compound, along with the trivalent



Scheme 1. Preparation of ligands L^2H_2 and L^3H_2 .



Scheme 2. Preparation of ligand L^4H and synthesis of complex L^4Co .

iron derivative $Fe[N(SiMe_3)_2]_3$. The cobalt amido compound's THF-free solid-state structure was determined to be a dimeric complex with bridging amido groups: $[(Me_3Si)_2NCo]_2(\mu-N(SiMe_3)_2)_2$ [30]. However, if the synthesis is conducted in THF, the resulting complex is monomeric with THF coordinated as a donor solvent [31]. The π -donor properties of the amido groups, combined with their steric bulk at distance from the metal center, afford a reactive complex with a coordinatively and sterically accessible metal center [32], and ligands especially amenable to protonolysis reactions.

Direct addition of the proligands L^2H_2 , L^3H_2 , and L^4H to $Co(N(SiMe_3)_2)_2 \cdot THF$ in THF results in an immediate color change from green to red, usually followed by precipitation of the corresponding ketoaminato cobalt complex from solution and isolation in high (80–90%) yields. The complexes are red to red-orange, and dissolve readily in THF or diethylether.

The solid state molecular structures of L^3Co and L^4Co have been determined, and are shown in Figs. 2 and 3 respectively. Structure and refinement data are listed in Table 1. The structures and observed metrical parameters are similar to those of other known cobalt(II) complexes with related ligands [20,21,33,34]. L^3Co exhibits a square planar geometry, with all the Co bond angles between 86.2 and 94.2°. There is a slight (8.5°) twisting of the N—Co—N and O—Co—O planes, presumably to accommodate the steric proximity of the phenyl rings

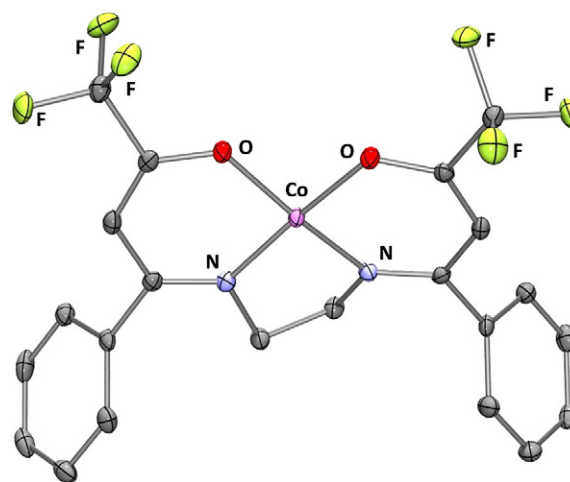


Fig. 2. Solid state molecular structure of L^3Co . Hydrogen atoms have been omitted for clarity. Selected bond lengths (Å); Co(1)—N(1) 1.8666, Co(1)—N(2) 1.8581, Co(1)—O(1) 1.8597, and Co(1)—O(2) 1.8609. Selected bond angles (°) N(2)—Co(1)—O(1) 173.91, N(2)—Co(1)—O(2) 93.66, O(1)—Co(1)—O(2) 86.23, N(2)—Co(1)—N(1) 86.54, O(1)—Co(1)—N(10) 94.16, and O(2)—Co(1)—N(1) 174.48.

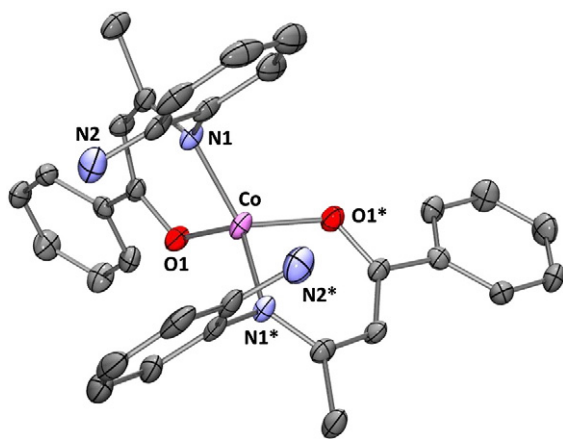


Fig. 3. Solid state molecular structure of L^1Co . Hydrogen atoms have been omitted for clarity. Selected bond lengths (Å); Co(1)—O(1) 1.9183(18) and Co(1)—N(1) 1.972(2). Selected bond angles ($^\circ$) N(1)—Co(1)—O(1) 94.67(8), O(1)—Co—O(1*) 109.82(12), N(1)—Co—N(1*) 115.89(13), and O(1)—Co—N(1*) 121.92(8).

and the CH_2CH_2 bridge. (A corresponding twist is absent in the related complex with $R_1 = CH_3$ and $R_2 = Ph$, where the phenyl groups are proximal to the O donor atoms rather than the N [33].) L^4Co exhibits a tetrahedral geometry and crystallographic C_2 symmetry, with intrachelate bite angles of $94.67(8)^\circ$ and interligand angles of $109.82(12)^\circ$ and $115.89(13)^\circ$. The twist angle between the chelate planes, as defined by the N—Co—O angle for each ligand, is slightly flattened at 82.4° . There is therefore little deviation from a tetrahedral geometry beyond that dictated by a $<100^\circ$ chelate bite angle. The Co atom lies 0.36 \AA above the mean OCCCN ligand plane, resulting in the two N-aryl groups being positioned such that the terminal NH_2 group of each ligand is positioned directly over the center of the N-aryl group of the other, with the two aryl rings only 3° away from being perfectly coplanar and a closest contact between the calculated position of the NH_2 hydrogen atoms and the aryl ring plane being 2.90 \AA . This distortion can be ascribed to a weak electronic π -stacking and NH_2 -aryl ring quadrupolar interactions in the solid state. As expected, the Co bond lengths are shorter in square planar L^3Co than in tetrahedral L^4Co , with the average Co—N shorter by 0.110 \AA and the average Co—O shorter by 0.058 \AA .

All these cobalt complexes exhibit broad, paramagnetically-shifted signals in their 1H NMR spectra, as expected for Co(II) in both square planar (low spin d^7 , $S = 1/2$) and tetrahedral (high spin d^7 , $S = 3/2$)

Table 1
Structure and refinement data for L^3Co and L^4Co .

| | L^3Co | L^4Co |
|---------------------------------------|---------------------------|------------------------|
| Crystal system | Monoclinic | Monoclinic |
| Formula | $C_{22}H_{18}F_6N_2O_2Co$ | $C_{32}H_{30}N_4O_2Co$ |
| Space group | P1 (#2) | C2/c (#15) |
| Formula weight | 513.30 | 561.53 |
| Lattice type | Primitive | C-centered |
| Crystal color/habit | Red/irregular | Red/needle |
| a/Å | 8.5442(2) | 17.357(1) |
| b/Å | 9.8498(3) | 10.1783(8) |
| c/Å | 12.5740(3) | 15.171(1) |
| α ($^\circ$) | 76.629(2) | 90 |
| β ($^\circ$) | 86.067(2) | 93.235(4) |
| γ ($^\circ$) | 80.055(2) | 90 |
| Z | | 4 |
| F_{000} | 518.00 | 1172.00 |
| λ (Mo K α)/ cm^{-1} | 0.71073 | 0.71073 |
| Reflections measured | 18636 | 19463 |
| Unique reflections | 4878 | 3363 |
| R_{int} | 0.036 | 0.074 |
| GoF | 1.07 | 1.03 |
| D_{cal} (g/cm^3) | 1.682 | 1.394 |

geometries. The selective modifications to the ligand substituents across a series of related compounds, combined with reliable integration values, permit a high degree of certainty in the assignment of signals despite their paramagnetic shifts. A comparison of the 1H NMR spectra of L^1Co , L^2Co , and L^3Co is shown in Fig. 4, along with peak assignments.

L^1Co bears a methyl substituent absent from L^2Co and L^3Co . The presence of the signal integrating for 6H at -20.8 ppm in the spectra of L^1Co , without a corresponding signal in the other two spectra, can therefore be assigned as that of the CH_3 groups. A weak signal common to all three compounds appears consistently between -60 and -95 ppm, and can be assigned to the ligand CH proton.¹ Other assignments can be determined similarly, and are listed in Table 2. Partial assignment of the spectrum of L^4Co can be made via comparison to those of other related tetrahedral bis(β -ketoamino) cobalt(II) complexes [34].

3.3. In vitro assays

The cytotoxic activities of four different cobalt complexes and their corresponding ligands were tested. Table 3 summarizes the data obtained by using six human cell lines of different origin, while Fig. 5 illustrates effects of two ligand/complex pairs on the PC-3 prostate cancer cell line. PC-3 cells were incubated for 48 h with the experimental drugs or DMSO vehicle. Viability of cells was assessed by the MTT (Fig. 5A) and the LDH (Fig. 5B) assays. With increasing concentration, both cobalt complexes L^1Co and L^2Co caused a concentration-dependent decrease in cell viability (Fig. 5A) and an increase in percentage of lysed cells (Fig. 5B). The corresponding ligands L^1H_2 and L^2H_2 had no effect according to both of these assays.

MTT assay results were selected for presentation in Table 3 due to the superior sensitivity of the assay (Fig. 5). Cells undergoing apoptosis during the initial prelytic stages release only low levels of LDH [35], which leads to underestimation of cell death according to the LDH assay (see Fig. 5 for example). Additional experiments were also performed to rule out possible interaction between reagents used in the LDH and MTT assays and the compounds (data not shown).

Table 3 shows the estimated EC_{50} values according to the MTT assay as well as the percentage of maximal inhibition observed at the concentration range of the compounds studied ($1-50 \mu M$). Data from experiments where statistically significant reduction of cell viability was observed are listed. The EC_{50} values were estimated as the concentration of a compound that induced toxicity halfway between the baseline and the maximum cytotoxic effect of a compound observed, which varied between 12% and 94% for the compounds studied. It is important to note that since only four different concentrations of the compounds were used, both the EC_{50} and maximal inhibition values shown in Table 3 are estimates, and more accurate values would require more detailed studies using additional concentration points. Similar to the effects of L^1Co illustrated in Fig. 5, LDH measurements often indicated higher EC_{50} values; however, effects of the compounds were similar in both LDH and MTT assays. Additionally, in several cases cells were counted under a microscope to confirm cytotoxicity of the compounds.

The data obtained identified several general trends (see Table 3). Firstly, cobalt complexes exhibit concentration-dependent activity against particular cells, and the complexes are more active than their corresponding ligands. In the majority of experiments, ligands did not exhibit any significant cytotoxic activity; in cases where they did, it was weaker than that of their corresponding cobalt complexes. Secondly, there is a significant difference among the effects of the four

¹ The CH signal is of low intensity and often so broad as to be undetectable, as is the case in the spectrum shown in Fig. 4. The 1H NMR spectrum of another square planar complex with $R^1 = CH_3$ and $R^2 = CF_3$ aids in and is consistent with these assignments: L. Gurley, W. S. McNeil, unpublished observations.

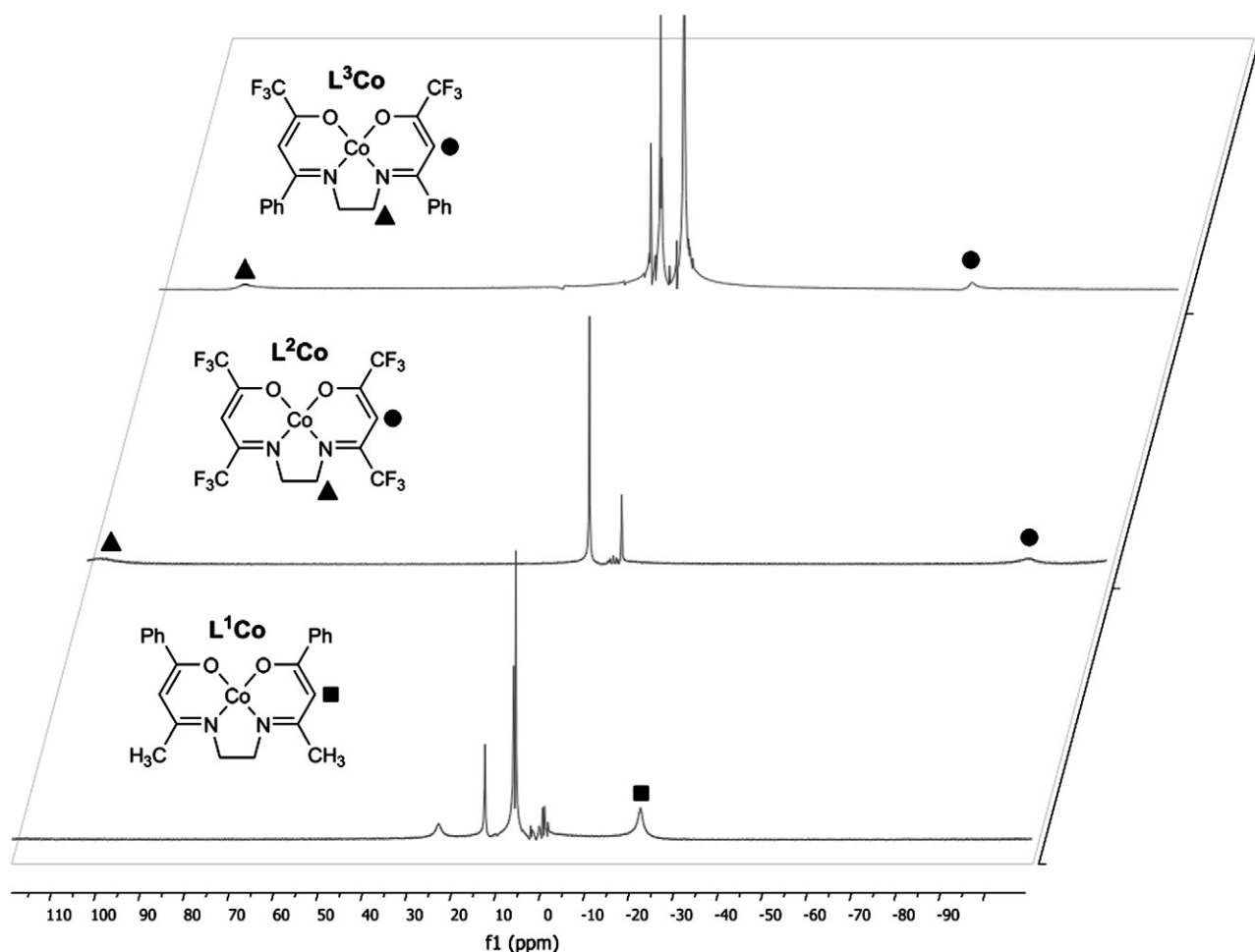


Fig. 4. Paramagnetic ^1H NMR spectra of L^1Co , L^2Co , and L^3Co .

cobalt complexes as measured by the EC_{50} and percent inhibition, with L^2Co being generally the most active and L^4Co the least active of the four compounds. Of particular note is the effect of L^2Co on PC3 cells, with 94% maximal inhibition and an EC_{50} of 2.5 μM . Thirdly, the cobalt complexes display selective activity against certain cell types. Two prostate cancer cell lines tested and THP-1 acute monocytic leukemia cells are consistently sensitive to the cobalt-containing drugs. Neuroblastoma, astrocytoma and hepatocellular carcinoma cells are not, with only weak activity exhibited by L^2Co against neuroblastoma cells, and by L^3Co and L^4Co against astrocytoma cells (Table 3). None of the compounds tested had significant effects on hepatocellular carcinoma cells.

These experiments indicate that some of the cobalt compounds exhibit cytotoxic activity against human tumor cells. Similar observations have been made by Klanicova et al. [36] who prepared $\text{Co}(\text{II})$ complexes with several N6-substituted adenine derivatives; five of their six cobalt complexes were active, while the corresponding ligands were not. Results from this study are similar to our data in that there was a significant variation in the activity of the different compounds towards

human osteogenic sarcoma cells. The range of EC_{50} values observed for this series of adenine compounds (7–28 μM) was very similar to that observed for the effects of our β -ketoaminato complexes on PC-3 (2.5–34 μM), VCaP (6–20 μM) and THP-1 (4–20 μM) cells (see Table 3). The cobalt-adenine complexes were not active against human MCF-7 breast cancer and K562 erythroleukemia cells. Only one of the complexes had a

Table 2
 ^1H NMR chemical shift data (ppm) for compounds L^1Co , L^2Co , L^3Co , and L^4Co .

| Compound | CH_3 | CH | CH_2 | Ph | NH_2 |
|-----------------------|---------------|-------|---------------|--|---------------|
| L^1Co | −20.8 | | −78.5 | 24.6, 14.2, 7.7 | |
| L^2Co | | 116.5 | −91.7 | | |
| L^3Co | | 101.0 | −62.8 | 29.4, 15.4 | |
| L^4Co | −19.2 | −34.8 | | 10.5, 14.7, 12.7, −11.0, −18.5, −26.5, −54.7 | 9.8 |

Table 3

Estimated EC_{50} and percentage maximal inhibition values of cobalt complexes and their respective ligands towards six different human cell lines.

| | PC3 | VCAP | THP-1 | SH-SY5Y | U-373 MG | HepG2 |
|------------------------|--------------------------|-------------------------------------|-------------------------|-------------------------|-------------------------|-------|
| L^1H_2 | NS ^a | 8 μM ^b 27% | NS | NS | NS | NS |
| L^1Co | 13 μM 67% | 20 μM 34% | 20 μM 58% | NS | NS | NS |
| L^2H_2 | NS | NS | NS | NS | NS | NS |
| L^2Co | 2.5 μM 94% | 6 μM 87% | 20 μM 39% | 20 μM 27% | NS | NS |
| L^3H_2 | NS | 2 μM 12% | NS | NS | NS | NS |
| L^3Co | 9 μM 88% | 13 μM 73% | 4 μM 19% | NS | 5 μM 15% | NS |
| L^4H_2 | 32 μM 34% | NS | 18 μM 64% | NS | NS | NS |
| L^4Co | 34 μM 38% | NS | 15 μM 83% | NS | 20 μM 28% | NS |

^a NS: no statistically significant effect compared to cells treated only with DMSO solvent.

^b Cytotoxicity was assessed after 48 h incubation as described in Fig. 5A for PC-3 cells and four of the compounds. EC_{50} values (μM) according to the MTT assay are presented as well as the percentage of maximal inhibition of cell viability.

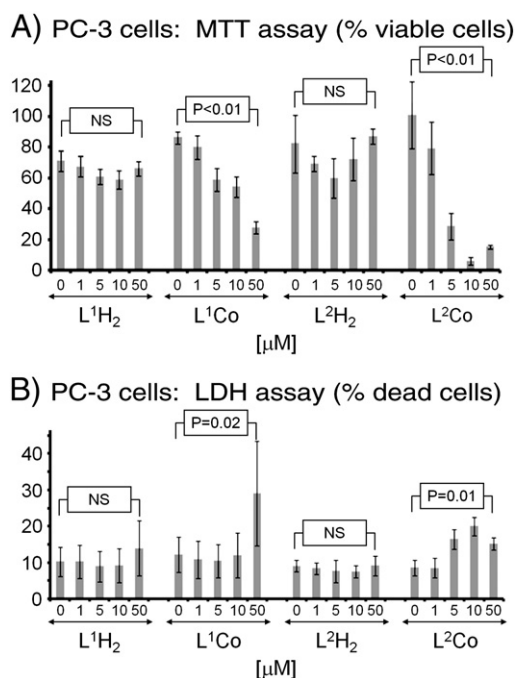


Fig. 5. Cobalt complexes L¹Co and L²Co reduce viability of human PC-3 prostate cancer cells, while their corresponding ligands L¹H₂ and L²H₂ are ineffective. PC-3 cells were seeded into 24-well plates at 1.2×10^5 cells per well in DMEM-F12 medium containing 5% FBS. Various concentrations (1–50 μM) of the two cobalt complexes or their respective ligands were added and cell viability assessed 48 h later by the MTT (A) and LDH (B) assays. Data (means ± SEM) from 4 independent experiments are presented as percent viable cells. The concentration-dependent effects of compounds were assessed by randomized block design ANOVA; NS, not significant.

weak effect ($EC_{50} = 42 \mu\text{M}$) towards G361 melanoma cells [36]. We observed similar cell-type specific activity of cobalt complexes, with notable effect on human prostate cancer and monocytic leukemia cells and weak or no effect on neuroblastoma, astrocytoma or hepatocellular carcinoma cells. Additional examples of cell type specificity were described for the complex of cobalt with mefenamic acid [37]; however, the EC_{50} values towards human MCF-7 breast cancer (94 μM), T-24 bladder cancer (27 μM), and A-549 non-small cell lung carcinoma (116 μM) were generally higher than those observed in our study. Cell type specific cytotoxic effects have been observed not only for Co(II) complexes but also for compounds containing a number of other metals, including Cu(II), Zn(II), Mn(II), Mo(VI), Ni(II), as well as Co(III) [37–40].

Selective alterations in the peripheral ligand substituents lead to changes in the cytotoxic activity of the cobalt complexes. The L²Co complex, which contains four trifluoromethyl groups, has the most potent cytotoxic activity toward prostate and monocytic leukemia cells. The two other square planar complexes L¹Co and L³Co exhibit lower potency, while L⁴Co is the least effective among the four cobalt complexes tested. L⁴Co is a Co(II) tetrahedral complex, which exhibits significant differences in its steric and electronic properties when compared to the other square planar β-ketoamine complexes. This is consistent with previous findings that tetrahedral cobalt(II) compounds with a 2-methylbenzimidazole ligand exhibit insignificant cytotoxicity toward a range of human cancer cell lines [39], suggesting that the relationship of cytotoxic activity to the geometry of four-coordinate cobalt(II) complexes is a general one. However, it should be noted that tetrahedral L⁴Co, along with L³Co, were the only two compounds that exhibit weak activity against U373-MG cells.

Ott et al. [11] have shown that modification of substituent on the alkyne ligand derived from acetylsalicylic acid leads to varying EC_{50} values of the obtained cobalt complexes towards human breast cancer cell lines. Very potent cytostatic effects were observed with EC_{50} reaching 1.4 μM for the lead compound in this series. It is noteworthy

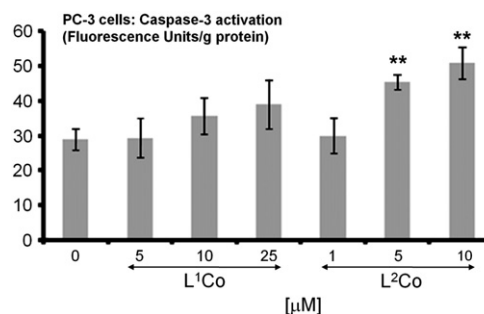


Fig. 6. Cobalt complex L²Co causes significant activation of caspase-3 in human PC-3 prostate cancer cells, while L¹Co has only a moderate effect. PC-3 cells (1.5×10^5 cells/mL) were exposed to various concentrations of L¹Co and L²Co or DMSO for 48 h. Caspase 3 activity was measured by a fluorometric assay. Data (means ± SEM) from four independent experiments are presented. **P<0.01, significantly different from cells exposed to the vehicle solution (DMSO) only, Fisher's LSD post hoc test.

that the widely used platinum-based chemotherapy agent, cisplatin, has been reported to have an EC_{50} value of 1–5 μM in different cell lines, including the prostate cancer cells [11,41]. This concentration range is very close to the EC_{50} of L²Co, as well as cobalt compounds described in previous studies [11,36,41]. It is also interesting to note that not all cobalt complexes exhibit the same cell specificity. For example, compounds described in this study were cytotoxic towards prostate cancer cell lines, while several acetylene(hexacarbonyl) dicobalt complexes described by Schmidt et al. [41] were toxic to two different human mammary tumor cell lines, with weak effects towards prostate cancer cells.

A series of experiments was performed to investigate possible mechanisms of action of the most active compounds. Fig. 6 illustrates that a 48 h incubation period with complex L²Co at concentrations of either 5 or 10 μM induces statistically significant activation of caspase-3 in PC-3 cells. Although there is also a concentration-dependent trend observed with L¹Co, the effect is weaker and does not reach statistical significance with the numbers of observations made ($n = 4$, $P = 0.068$ at 25 μM, Fisher's LSD *post hoc* test).

The effects of two MAP kinase inhibitors were examined. Fig. 7 illustrates that SP600125, a selective JNK inhibitor, at 20 μM significantly reduces the activity of L¹Co, L²Co, and L³Co against PC-3 cells. The effect of PD98059, an MEK1/2 inhibitor, is weaker and reaches statistical significance ($P < 0.05$) only in the case of L¹Co. Different concentrations

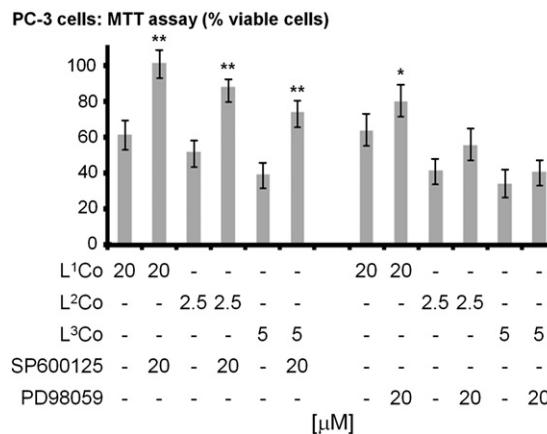


Fig. 7. Cytotoxicity of cobalt complexes towards human PC-3 prostate cancer cells is reduced by JNK and MAPK/ERK kinase inhibitors. PC-3 cells were pre-incubated for 15 min with 20 μM of either SP600125, a selective JNK inhibitor, or PD98059, a selective MAPK/ERK kinase inhibitor, before being exposed to three different cobalt complexes. Cell viability was assessed 48 h later by the MTT assay. Data (means ± SEM) from 5 independent experiments are expressed as percent viable cells. *P<0.05; **P<0.01 significantly different from cells treated with the cobalt complex only; paired Student's *t*-test values were corrected for multiple comparisons by Holm's step-down procedure.

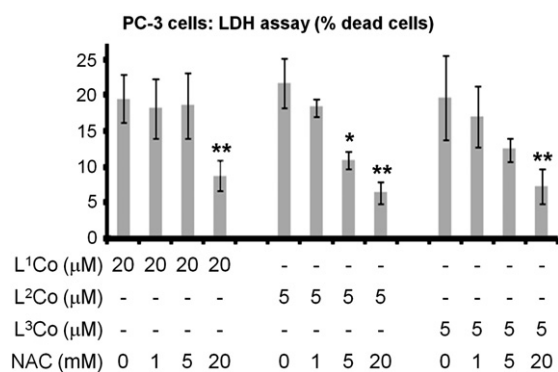


Fig. 8. Antioxidant NAC reduces cytotoxicity of cobalt complexes towards human PC-3 prostate cancer cells. PC-3 cells were pre-incubated for 15 min with various concentrations of NAC before being exposed to three different cobalt complexes. Cell viability was assessed 48 h later by the LDH assay. Data (means \pm SEM) from 3 to 6 independent experiments are expressed as percent dead cells. * $P < 0.05$; ** $P < 0.01$ significantly different from cells treated with the cobalt complex only, Fisher's LSD post hoc test.

of the cobalt complexes were used to induce PC-3 cell death; these concentrations were established in the preliminary experiments in order to achieve similar levels of activity among the three different compounds.

Similarly, NAC, a potent thiol antioxidant, prevents cytotoxic activity induced by the three cobalt complexes in a concentration-dependent manner (Fig. 8). Again, preliminary experiments helped establish concentrations of the cobalt complexes needed to achieve similar levels of activity according to the LDH assay. The MTT assay was not used for these experiments due to an interaction of NAC with the formazan dye. NAC did not interfere with the LDH assay.

These experiments reveal several similarities with the mode of action exhibited by cisplatin and other anti-cancer drugs (for reviews see [16,42]), which may suggest that the cell death induced by cobalt compounds is at least partially a result of apoptosis. The increased caspase-3 activation by L²Co, and to a lesser extent by L¹Co (Fig. 6), is a common mechanism of action for many anti-cancer drugs [42] including cisplatin [43]. As well, the PC-3 cell death caused by three of the most active cobalt compounds (L¹Co, L²Co, and L³Co) appears dependent on activation of MAP kinases, and JNK in particular, a mechanism that has also been widely implicated in apoptosis as induced by cisplatin and other anti-cancer drugs [12,44].

It has also been shown that oxidative stress is caused by a number of anti-cancer medications including cisplatin [45], and the observed reduction of cytotoxic activity upon treatment with NAC indicates that the generation of reactive oxygen species could also be an active mechanism of activity of the cobalt complexes [13].

4. Conclusions

Four (β -ketoamino)cobalt compounds and their corresponding organic ligands have been tested for their cytotoxic effects against six human cancer cell lines. The data indicate that some of these cobalt compounds, L²Co in particular, could be useful as anti-tumor agents, and that the activity is selective towards prostate cancer and leukemia cells. Initial experiments revealed some of the molecular mechanisms engaged by these novel compounds, including caspase-3 and MAP kinase activation as well as oxidative stress, but further work will be needed to fully characterize the cell signaling pathways engaged by the cobalt complexes. Future work will also attempt to increase the potency and selectivity of the cobalt-containing drugs towards, for example, prostate cancer cells through systematic derivatization of the ligands used for preparation of the cobalt complexes.

Abbreviations

ANOVA analysis of variance
DMF N,N-dimethyl formamide

DMSO dimethylsulfoxide
EC₅₀ half-maximal effective concentration
ERK extracellular signal-regulated kinase
FBS fetal bovine serum
JNK c-Jun NH2-terminal kinase
LDH lactate dehydrogenase
LSD least significant differences
MAPK mitogen-activated protein kinase
MEK1/2 MAPK/ERK kinase
MTT 3-(4,5-dimethylthiazol-2-yl)-2,5-diphenyltetrazolium bromide
NAC N-acetyl-L-cysteine
NMR nuclear magnetic resonance
NS not significant
SDS sodium dodecyl sulfate
TBDMS *tert*-butyldimethylsilyl, *t*BuMe₂Si
THF tetrahydrofuran

Acknowledgements

This work was supported by grants from the Natural Sciences and Engineering Research Council of Canada, the Jack Brown and Family Alzheimer's Disease Research Foundation, Prostate Cancer Canada, and the Irving K. Barber School of Arts and Sciences at UBC Okanagan. The authors would like to thank Ms. Jocelyn Madeira for the technical assistance and Dr. Brian Patrick for the X-ray crystallographic analysis.

Appendix A. Supplementary data

Supplementary data to this article can be found online at doi:10.1016/j.jinorgbio.2011.03.005.

References

- [1] K.H. Thompson, C. Orvig, *Science* 300 (2003) 936–939.
- [2] E.R. Jamieson, S.J. Lippard, *Chem. Rev.* 99 (1999) 2467–2498.
- [3] D.J. Vaughn, G.A. Gignac, A.T. Meadows, *Ann. Intern. Med.* 136 (2002) 463–470.
- [4] S. van Zutphen, J. Reedijk, *Coord. Chem. Rev.* 249 (2005) 2845–2853.
- [5] A.S. Abu-Surrah, M. Kettunen, *Curr. Med. Chem.* 13 (2006) 1337–1357.
- [6] M. Knipp, *Curr. Med. Chem.* 16 (2009) 522–537.
- [7] A.M. Montana, C. Batalla, *Curr. Med. Chem.* 16 (2009) 2235–2260.
- [8] G. Cossa, L. Gatti, F. Zunino, P. Perego, *Curr. Med. Chem.* 16 (2009) 2355–2365.
- [9] R. Banerjee, S.W. Ragsdale, *Annu. Rev. Biochem.* 72 (2003) 209–247.
- [10] T. Yano, T. Ozawa, H. Masuda, *Chem. Lett.* 37 (2008) 672–677.
- [11] I. Ott, K. Schmidt, B. Kircher, P. Schumacher, T. Wiglenda, R. Gust, *J. Med. Chem.* 48 (2005) 622–629.
- [12] I. Ott, B. Kircher, R. Dembinski, R. Gust, *Expert Opin. Ther. Pat.* 18 (2008) 327–337.
- [13] J.A. Schwartz, E.K. Lium, S.J. Silverstein, *J. Virol.* 75 (2001) 4117–4128.
- [14] W.K. Hagmann, *J. Med. Chem.* 51 (2008) 4359–4369.
- [15] D. O'Hagan, D.B. Harper, *J. Fluorine Chem.* 100 (1999) 127–133.
- [16] R. Kim, K. Tanabe, Y. Uchida, M. Emi, H. Inoue, T. Toge, *Cancer Chemother. Pharmacol.* 50 (2002) 343–352.
- [17] G. Tortora, R. Bianco, G. Daniele, F. Ciardiello, J.A. McCubrey, M.R. Ricciardi, L. Ciuffreda, F. Cognetti, A. Tafuri, M. Milella, *Drug Resist. Updat.* 10 (2007) 81–100.
- [18] Y.H. Kang, M.J. Yi, M.J. Kim, M.T. Park, S. Bae, C.M. Kang, C.K. Cho, I.C. Park, M.J. Park, C. H. Rhee, S.I. Hong, H.Y. Chung, Y.S. Lee, S.J. Lee, *Cancer Res.* 64 (2004) 8960–8967.
- [19] P.J. McCarthy, R.J. Hovey, K. Ueno, A.E. Martell, *J. Am. Chem. Soc.* 77 (1955) 5820–5824.
- [20] S.Z. Haider, A. Hashem, K.M.A. Malik, M.B. Hursthouse, *J. Bangladesh Acad. Sci.* 4 (1980) 139–150.
- [21] W.T. Robinson, G.A. Rodley, *Acta Crystallogr. Sect. A* 28 (1972) S52.
- [22] H. Burger, U. Wannagat, *Monatsh. Chem.* 94 (1963) 1007–1012.
- [23] J.A.T. Norman, Air Products and Chemicals, Inc., USA. Patent Application: EP, 1991, p. 17.
- [24] P.R. Shipley, C.C.A. Donnelly, C.H. Le, A.D. Bernauer, A. Klegeris, *Int. J. Mol. Med.* 24 (2009) 711–715.
- [25] M.M. Bradford, *Anal. Biochem.* 72 (1976) 248–254.
- [26] A.M. Youssef, E.G. Neeland, E.B. Villanueva, M.S. White, I.M. El-Ashmawy, B. Patrick, A. Klegeris, A.S. Abd-El-Aziz, *Bioorg. Med. Chem.* 18 (2010) 5685–5696.
- [27] S. Holm, *Scand. J. Stat.* 6 (1979) 65–70.
- [28] A.E. Martell, R.L. Belford, M. Calvin, *J. Inorg. Nucl. Chem.* 5 (1958) 170–181.
- [29] M.F. Richardson, R.E. Sievers, *J. Inorg. Nucl. Chem.* 32 (1970) 1895–1906.
- [30] B.D. Murray, P.P. Power, *Inorg. Chem.* 23 (1984) 4584–4588.
- [31] S.D. Reid, A.J. Blake, C. Wilson, J.B. Love, *Inorg. Chem.* 45 (2006) 636–643.

- [32] P.L. Holland, *Acc. Chem. Res.* 41 (2008) 905–914.
- [33] S. Brückner, M. Calligaris, G. Nardin, L. Randaccio, *Inorg. Chim. Acta* 2 (1968) 379–385.
- [34] K.C.D. Robson, C.D. Phillips, B.O. Patrick, W.S. McNeil, *Dalton Trans.* 39 (2010) 2573–2578.
- [35] E. Bonfoco, D. Krainc, M. Ankarcona, P. Nicotera, S.A. Lipton, *Proc. Natl. Acad. Sci. U.S.A.* 92 (1995) 7162–7166.
- [36] A. Klanicova, Z. Travnicek, I. Popa, M. Cajan, K. Dolezal, *Polyhedron* 25 (2006) 1421–1432.
- [37] D. Kovala-Demertzi, D. Hadjipavlou-Litina, M. Staninska, A. Primikiri, C. Kotoglou, M.A. Demertzis, *J. Enzyme Inhib. Med. Chem.* 24 (2009) 742–752.
- [38] N. Katsaros, M. Katsarou, S.P. Sovilj, K. Babic-Samardzija, D.M. Mitic, *Bioinorg. Chem. Appl.* 2 (2004) 193–207.
- [39] O. Sanchez-Guadarrama, H. Lopez-Sandoval, F. Sanchez-Bartez, I. Gracia-Mora, H. Hopfl, N. Barba-Behrens, *J. Inorg. Biochem.* 103 (2009) 1204–1213.
- [40] Z.C. He, D.N. Lai, L.P.G. Wakelin, *Eur. J. Pharmacol.* 637 (2010) 11–15.
- [41] K. Schmidt, M. Jung, R. Keilitz, B. Schnurr, R. Gust, *Inorg. Chim. Acta* 306 (2000) 6–16.
- [42] Z.H. Siddik, *Cancer Treat. Res.* 112 (2002) 263–284.
- [43] B. Del Bello, D. Moretti, A. Gamberucci, E. Maellaro, *Oncogene* 26 (2007) 2717–2726.
- [44] A. Brozovic, M. Osmak, *Cancer Lett.* 251 (2007) 1–16.
- [45] D.M. Mattson, M.A. Iman, D. Dayal, A.D. Parsons, N. Aykin-Burns, L. Li, K.P. Orcutt, D.R. Spitz, K.J. Dornfeld, A.L. Simons, *Free Radical Biol. Med.* 46 (2009) 232–237.